THE JOURNAL OF BIOLOGICAL CHEMISTRY VOL. 289, NO. 45, pp. 31188–31199, November 7, 2014

Different Interaction Modes for Protein-disulfide Isomerase (PDI) as an Efficient Regulator and a Specific Substrate of Endoplasmic Reticulum Oxidoreductin-1α (Ero1α)*

Received for publication, August 5, 2014, and in revised form, September 5, 2014 Published, JBC Papers in Press, September 25, 2014, DOI 10.1074/jbc.M114.602961

Lihui Zhang[‡§1], **Yingbo Niu**[‡§1], **Li Zhu**[‡§], **Jingqi Fang**[‡§], **Xi'e Wang**[‡], **Lei Wang**[‡2], **and Chih-chen Wang**[‡3]

From the [‡]*National Laboratory of Biomacromolecules, Institute of Biophysics, Chinese Academy of Sciences, Beijing 100101, China and* [§]*University of Chinese Academy of Sciences, Beijing 100049, China*

Background: Ero1α and PDI constitute the pivotal oxidative protein folding pathway in mammalian ER.
Results: Both catalytic domains of PDI and PDI homologues rapidly regulate Ero1α activity while Ero1α asymmetrically oxidizes PDI.
Conclusion: The modes for PDI as efficient regulator and specific substrate of Ero1α are different.
Significance: This study reveals how Ero1α-PDI interplay ensures oxidative protein folding homeostatically.

Protein-disulfide isomerase (PDI) and sulfhydryl oxidase endoplasmic reticulum oxidoreductin-1α (Ero1α) constitute the pivotal pathway for oxidative protein folding in the mammalian endoplasmic reticulum (ER). Ero1α oxidizes PDI to introduce disulfides into substrates, and PDI can feedback-regulate Ero1α activity. Here, we show the regulatory disulfide of Ero1α responds to the redox fluctuation in ER very sensitively, relying on the availability of redox active PDI. The regulation of Ero1α is rapidly facilitated by either *a* or *a*′ catalytic domain of PDI, independent of the substrate binding domain. On the other hand, activated Ero1α specifically binds to PDI via hydrophobic interactions and preferentially catalyzes the oxidation of domain *a*′. This asymmetry ensures PDI to function simultaneously as an oxidoreductase and an isomerase. In addition, several PDI family members are also characterized to be potent regulators of Ero1α. The novel modes for PDI as a competent regulator and a specific substrate of Ero1α govern efficient and faithful oxidative protein folding and maintain the ER redox homeostasis.

Disulfide bonds play important roles in the structure and function of many secretory and membrane proteins. The correct formation of disulfides during the folding of nascent peptides to native proteins, namely oxidative protein folding, takes place mainly in the endoplasmic reticulum (ER)[4] in eukaryotic cells (1). Protein-disulfide isomerase (PDI) and sulfhydryl oxidase ER oxidoreductin-1 (Ero1) constitute the pivotal pathway for oxidative protein folding from yeast to mammals. PDI contains four thioredoxin (Trx) domains arranged as *a-b-b*′*-a*′, with two -CGHC- active sites respectively located in domain *a* and *a*′. PDI can directly catalyze disulfide formation in reduced substrates, as well as the isomerization reaction to convert aberrant disulfides to correct ones (2). Ero1 flavoproteins can catalyze the re-oxidation of reduced PDI for continuous transfer of disulfides to substrate proteins. The -CXXXXC- outer active site located in an intrinsically flexible loop of Ero1 transfers electrons from the active site of PDI to the buried -CXXC- inner active site, and the electrons are then used to reduce oxygen into hydrogen peroxide via flavin adenine dinucleotide cofactor (3, 4).

There are two isoforms of Ero1 in mammalian cells: Ero1α is widely expressed (5) and Ero1β is abundantly expressed in select secretory tissues such as the pancreas (6). Both Ero1α and Ero1β activities are regulated by regulatory disulfides formed between catalytic and non-catalytic cysteines to avoid futile oxidation cycles with excess hydrogen peroxide production (7–9). For Ero1α particularly, the formation of two regulatory disulfides Cys94-Cys131 and Cys99-Cys104 in the inactive resting state blocks disulfide transferring from the inner active site (Cys394-Cys397) to PDI via the outer active site (Cys94-Cys99). These two regulatory disulfides need to be reduced to liberate the outer active site for activation of Ero1α. A conserved long-range disulfide Cys85-Cys391 was suggested to also participate in the activity regulation of Ero1α (7, 8), which was challenged later (10).

In cells, the poise of active and inactive Ero1α at steady state was demonstrated to be dependent on the level of PDI (7, 11). Thus, PDI seems not only a substrate but also a physiological regulator of its oxidase Ero1α. However, the dynamics of the transition between active and inactive Ero1α during the fluctuation of ER redox environment and the role of PDI in these processes remain largely unknown. For the interplay between Ero1α and PDI, it has been elucidated that the catalytic active Ero1α preferentially oxidizes the C-terminal active site in domain *a*′ of PDI, rather than the N-terminal active site in

* This work was supported by grants from the Chinese Ministry of Science and Technology (2011CB910303 and 2012CB911002, to C. C. W.) and National Natural Science Foundation of China (31370775, to L. W.).
[1] These authors contributed equally to this work.
[2] To whom correspondence may be addressed: National Laboratory of Biomacromolecules, Institute of Biophysics, Chinese Academy of Sciences, 15 Datun Road, Chaoyang District, Beijing 100101, China. Tel.: +86-10-64888501; Fax: +86-10-64840672; E-mail: wanglei@moon.ibp.ac.cn.
[3] To whom correspondence may be addressed: National Laboratory of Biomacromolecules, Institute of Biophysics, Chinese Academy of Sciences, 15 Datun Road, Chaoyang District, Beijing 100101, China. Tel.: +86-10-64888500; Fax: +86-10-64840672; E-mail: chihwang@sun5.ibp.ac.cn.
[4] The abbreviations used are: ER, endoplasmic reticulum; ANS, 1-anilinonaphthalene-8-sulphonate; BPTI, bovine pancreatic trypsin inhibitor; Ero1α, endoplasmic reticulum oxidoreductin-1α; GSH, reduced glutathione; GSSG, oxidized glutathione; mPEG-5k, methoxy polyethyleneglycol 5000 maleimide; NEM, *N*-ethylmaleimide; PDI, protein-disulfide isomerase; Trx, thioredoxin; UPR, unfolded protein response.

domain *a* (8, 12), although the reduction potentials of the two active sites are very similar (13). Also we and others have provided evidence that the primary substrate binding domain *b′* of PDI plays a critical role in binding with Ero1α for functional disulfide relay (10, 12, 14). On the other hand, the molecular mechanism of the reduction/oxidation of the regulatory disulfides of Ero1α by PDI is little understood. There are at least twenty PDI family members (PDIs) in mammalian ER (2), but Ero1α as well as its hyperactive isoform Ero1β poorly catalyzes the oxidation of other PDIs (9, 15). Meanwhile other PDIs at steady state unsuccessfully modulate the redox states of Ero1α (15). Altogether, to reveal the molecular mechanism underlying the interplay between Ero1α and PDIs is central and crucial for understanding how efficient oxidative folding and redox balance in the ER are maintained in mammalian cells.

In this study, we report that (i) Cys85-Cys391 disulfide in Ero1α is stable and remains intact during the physiological activation of the enzyme; (ii) Cys94-Cys131 regulatory disulfide responds to the redox fluctuation in ER very sensitively, and its reduction/oxidation can be facilitated by not only PDI but also some other PDIs; (iii) either catalytic domain of PDI is able to facilitate the regulation of Ero1α, and the substrate binding domain *b′* of PDI is not essential for activation/inactivation of Ero1α; (iv) the functional oxidation of PDI catalyzed by Ero1α is asymmetric to make the *a′* domain act primarily as an oxidase and the *a* domain as an isomerase. The above findings shed great light on the mechanism underlying the interplay between Ero1α and PDI proteins, which ensures the efficiency and fidelity of oxidative protein folding and maintains the thiol-disulfide redox homeostasis in the ER.

EXPERIMENTAL PROCEDURES

Plasmid Construction and Protein Preparation—For protein expression in bacteria, pGEX-6P-1 plasmids encoding Ero1α WT and Ero1α C104/131A were used as previously described (9). pET28a-Ero1p (Phe56-Leu424) was kindly donated by Dr. Yi Yang (East China University of Science and Technology, China). pQE30 plasmids encoding PDI WT, PDI C1, PDI C2, and PDI C1/2 (12), PDI *a* and PDI *a′c* (16) were laboratory products. pET23b-PDIp, pET23b-P5, pET23b-ERp18, pET23b-ERp72, and pET23b-Pdi1p were generous gifts from Dr. Lloyd W. Ruddock (University of Oulu, Finland). pET15b-ERp46 and pQE30-ERp57 were kindly provided by Dr. Xi Wang (this laboratory). Chimeric PDI-PDIs proteins were constructed by fusing the catalytic domain of PDIp *a′* (Leu377-Leu525), ERp57 *a′* (Lys366-Leu505), ERp72 *a′* (Lys515-Leu645), P5 a^1 (Gly144-Glu280), and ERp46 a^2 (Asp320-Leu432) to the C terminus of PDI *bb′* base (Ala136-Leu355), and inserted into pQE30 vector at BamHI/HindIII sites. For expression in mammalian cells, pcDNA3.1-PDI, pcDNA3.1-Ero1α-myc, and pcDNA3.1-Ero1α-HA were used as described (17). pcDNA3.1-HA-PDI was generated by insertion of an HA tag after the N-terminal ER signal sequence. An aspartic acid residue was inserted before the tag to recreate the signal sequence cleavage site. The cDNA encoding P5 with its signal sequence, a C-terminal myc tag followed by an ER-retrieval motif (KDEL), and a KpnI restriction site on the upstream of the myc epitope, was generated by PCR and inserted into pcDNA3.1 vector at XbaI/HindIII sites. The cDNA for PDIp, ERp18, ERp72, and ERp57 with their own signal sequences and ERp46 with PDI's signal sequence were amplified by PCR and ligated into XbaI/KpnI digested pcDNA3.1-P5-myc. All the other mutations for Ero1α, PDI, Ero1p and Pdi1p were created using the Fast Mutagenesis System (TransGen) and verified by DNA sequencing (Invitrogen).

Recombinant Ero1p (18) and Ero1α (12) proteins were expressed and purified as described. PDI proteins and Pdi1p proteins were purified as for PDI (19). For reduced protein preparation, PDI proteins at 100 μM or Ero1α at 10 μM with 100 mM DTT and Pdi1p proteins at 100 μM with 10 mM GSH were incubated in buffer A (50 mM Tris-HCl, 150 mM NaCl, 2 mM EDTA, pH 7.6) for 1 h at 25 °C. Excess reductants were then removed using a HiTrap desalting column (GE Healthcare) pre-equilibrated with buffer A, and the reduced proteins were kept on ice for use only in the same day. For oxidized protein preparation, PDI proteins at 100 μM or Ero1α at 50 μM was incubated with 50 mM potassium ferricyanide in buffer A for 1 h at 25 °C, and then chromatographed through a Superdex-200 10/300 GL column (GE Healthcare) pre-equilibrated with buffer A. Monomeric protein fraction was collected, concentrated and stored at −80 °C in aliquots.

Cell Culture, Transfection, and Antibodies—HeLa cells were cultured in DMEM (Invitrogen) containing 5% fetal bovine serum, 100 units/ml penicillin and 100 μg/ml streptomycin (Invitrogen) at 5% CO_2. Plasmids were transfected using Lipofectamine 2000 (Invitrogen) according to the manufacturer's instructions. After 48 h, the transfected cells were harvested, or as needed treated with 50 μM DTT and 50 μM 16F16 (Sigma-Aldrich) dissolved in DMSO for 8 h before harvest.

The following mouse monoclonal antibodies were used: αEro1α (2G4, a gift from Roberto Sitia, Università Vita-Salute San Raffaele, Italy), αEro1α (ab57177, Abcam), αPDI (RL90, Abcam), αGAPDH (GAPDH-71.1, Sigma-Aldrich), αmyc (9E10, Sigma-Aldrich), and αHA (HA-7, Sigma-Aldrich).

RNA Interference—The pSUPER-retro-puro vector (Oligoengine) expressing the shRNA targeting PDI sequence 5′-GAGTGTGTCTGACTATGAC-3′ (20) was constructed according to the manufacturer's instructions. The pSUPER-shEro1α plasmid was used as described (17). pSUPER plasmids were transiently transfected into HeLa cells on day 1. Puromycin was added into the culture medium to a final concentration of 2 μg/ml on day 2 to kill the negative cells. Then pSUPER plasmids were co-transfected with pcDNA3.1-Ero1α C99/104A on day 3. Cells were harvested on day 5.

Assay for the in Vivo Redox States of Ero1α, Immunoprecipitation, and Western Blotting—For Ero1α activation, the harvested cells were re-suspended in DMEM containing 150 μM DTT at 25 °C. Aliquots were taken and immediately blocked by 20 mM *N*-ethylmaleimide (NEM, Sigma-Aldrich) at different times to trap disulfide bonds. For Ero1α inactivation, after incubation with 10 mM DTT in DMEM at 25 °C for 10 min, cells were quickly washed twice by ice-cold phosphate-buffered saline to remove excess DTT and re-suspended in DMEM at 25 °C. Aliquots were then taken and immediately blocked by 20 mM NEM at different times. Cells were lysed in radio immunoprecipitation assay buffer (Beyotime) containing 1 mM phenylmethanesulfonyl fluoride and 20 mM NEM. Post-nuclear super-

natants were resolved by nonreducing SDS-PAGE to analyze the redox states of Ero1α. Immunoprecipitation was carried out by incubation of cell lysates with αHA for 2 h at 4 °C, followed by addition of protein A + G Agarose (Beyotime) and rotation for another 2 h at 4 °C. The beads were then washed for 3 times with RIPA buffer and the resuspended samples were analyzed by nonreducing SDS-PAGE. Proteins were transferred to polyvinylidene difluoride membranes (Millipore) using a semi-dry transfer apparatus, and the membranes were blocked in 5% milk and decorated by antibodies and enhanced chemiluminescence (Thermo Scientific), and visualized by using a ChemiScope mini imaging system (Clinx Science).

Redox State Determination of Activated and Inactivated Ero1α in Vitro—For the activation of Ero1α, oxidized Ero1α was either incubated with 10-fold reduced PDI proteins or treated by 10-fold PDI proteins in the presence of GSH/GSSG at different ratios. For the inactivation of Ero1α, reduced Ero1α was mixed with 10-fold oxidized PDI proteins. To study the self-oxidation of Ero1α, reduced Ero1α proteins were incubated with equimolar GST-Ero1α proteins. All experiments were carried out in buffer A at 25 °C, and aliquots were taken at different times and immediately quenched with 20 mM NEM. The samples were then analyzed by nonreducing SDS-PAGE followed by immunoblotting with αEro1α. Band intensity was quantified using Image J software (National Institutes of Health).

Oxygen Consumption Assay—Oxygen consumption was measured at 25 °C using an Oxygraph Clark-type oxygen electrode (Hansatech Instruments) as described (9). Briefly, reactions were initiated by adding Ero1 proteins to a final concentration of 2 μM into buffer B (100 mM Tris-HAc, 50 mM NaCl, 2 mM EDTA, pH 8.0) containing 20 μM PDI proteins and various concentrations of GSH and GSSG.

Gel-based PDI Oxidation Assay—Oxidation of 20 μM reduced PDI proteins by 3 μM Ero1 proteins were carried out at 25 °C in buffer B. At different time points, aliquots were taken for immediate mixing with equal volume of 2× SDS-PAGE loading buffer containing 5 mM mPEG-5k (Sigma-Aldrich) followed by incubation at 33 °C for 20 min. The samples were subjected to SDS-PAGE after consuming excess of mPEG-5k by 25 mM DTT.

PDI Isomerase Activity Assay—Scrambled bovine pancreatic RNase A (Sigma-Aldrich) was prepared as described (21). Ero1 and PDI proteins at equimolar were pre-incubated at 25 °C for 30 min in buffer B, and the isomerase activities of PDI proteins at 3 μM were then assayed by adding scrambled RNase A and cCMP (Sigma-Aldrich) to a final concentration of 8 μM and 4.5 mM, respectively. The absorbance increase at 296 nm due to the hydrolysis of cCMP by refolded RNase A was monitored at 25 °C, and the concentration of reactivated RNase A was calculated with details described elsewhere (22). The linear slope of RNase A reactivation was taken as the isomerase activity of PDI.

BPTI Oxidative Folding Assay—BPTI (Sigma-Aldrich) of 2.5 mg was denatured and reduced by incubation with 20 mM DTT and 6 M guanidine hydrochloride in 0.1 M Tris-HCl (pH 8.0) at 50 °C for 5 h. Excess reductants and denaturants were removed using a HiTrap desalting column pre-equilibrated with 0.01 M HCl. The refolding assays were carried out at 25 °C by adding denatured and reduced BPTI to a final concentration of 30 μM into buffer B containing pre-incubated Ero1 and PDI proteins making a final concentration of 3 μM of each. Aliquots were taken at different time points and quenched by adding 0.1 volumes of 5 M HCl. The samples were then loaded onto a Vydac C18 analytical HPLC column (250 × 4.6 mm, GRACE) and eluted with a flow rate of 1 ml/min using a linear gradient of acetonitrile from 15% to 50% at a rate of 0.7%/min in 0.05% trifluoroacetic acid. The absorbance at 229 nm was monitored. The percentage of each folding intermediate during the refolding was quantified using Chromeleon software (Thermo Scientific).

RESULTS

Cys85-Cys391 Remains Intact during Ero1α Activation—Ero1α contains fifteen cysteine residues with the disulfide pattern as shown in Fig. 1*A* (7, 14, 23). First, we checked the controversial regulatory function of Cys85-Cys391 by taking advantage of retarded protein mobility on nonreducing SDS-PAGE caused by long-range disulfide breakage. Three Ero1α Cys-to-Ala mutants C85/391A, C104/131A, and C85/104/131/391A were prepared to serve as a disulfide ruler, mimicking the reduction of long-range disulfide of Cys85-Cys391, Cys94-Cys131, and the both, respectively (23). As shown in Fig. 1*B*, purified recombinant Ero1α wild-type (WT) migrated exclusively as oxidized state (Ox2, lane 1), and Ero1α C104/131A migrated slower (Ox1, lane 11). Ero1α C85/C391A migrated a little faster than the Ox1 form (lane 10). Disruption of the two long-range disulfides (Cys94-Cys131 and Cys85-Cys391) made the migration much slower (lane 12) close to the reduced form (red, lane 13). Glutathione (GSH) alone did not reduce Ero1α, while in the presence of PDI, the physiological substrate of Ero1α, the slower migrating species (Ox1) in Ero1α WT gradually emerged with increasing ratios of reduced to oxidized glutathione (GSH/GSSG). This species migrated the same as C104/131A but slightly slower than C85/391A, implying that the long-range disulfide of Cys94-Cys131 was reduced. At 10 mM GSH, the majority of Ero1α shifted to Ox1 state but no band at the mobility of C85/104/131/391A was observed, indicating that Cys85-Cys391 was still intact after the reduction of Cys94-Cys131. Oxygen consumption assays confirmed that the Ox1 species is enzymatically active (Fig. 1*C*), indicating that the reduction of Cys94-Cys131 results in the activation of Ero1α. Correspondingly, C85/391A (with intact Cys94-Cys131 disulfide) was reduced by PDI and GSH to a slower migrating band, but C104/131A (with intact Cys85-Cys391) was not reduced (Fig. 1*D*), suggesting that Cys85-Cys391 is very stable.

We next examined the influence of PDI on the redox states of Ero1α in HeLa cells. Ero1α C99/104A mutant was used because this mutant retains both long-range disulfides of Cys85-Cys391 and Cys94-Cys131 for redox state examination but lacks intact outer active site (Cys94-Cys99) for catalyzing substrate oxidation, so that the interference from the re-oxidation of Ero1α regulatory disulfides by oxidized substrates can be excluded. As shown in Fig. 1*E*, Ero1α C99/104A migrated in both Ox1 and Ox2 forms, implying that in cells it exists in both activated and inactivated forms, similar to Ero1α WT. Co-expression of PDI at steady state led to moderate but significant increase of Ox1

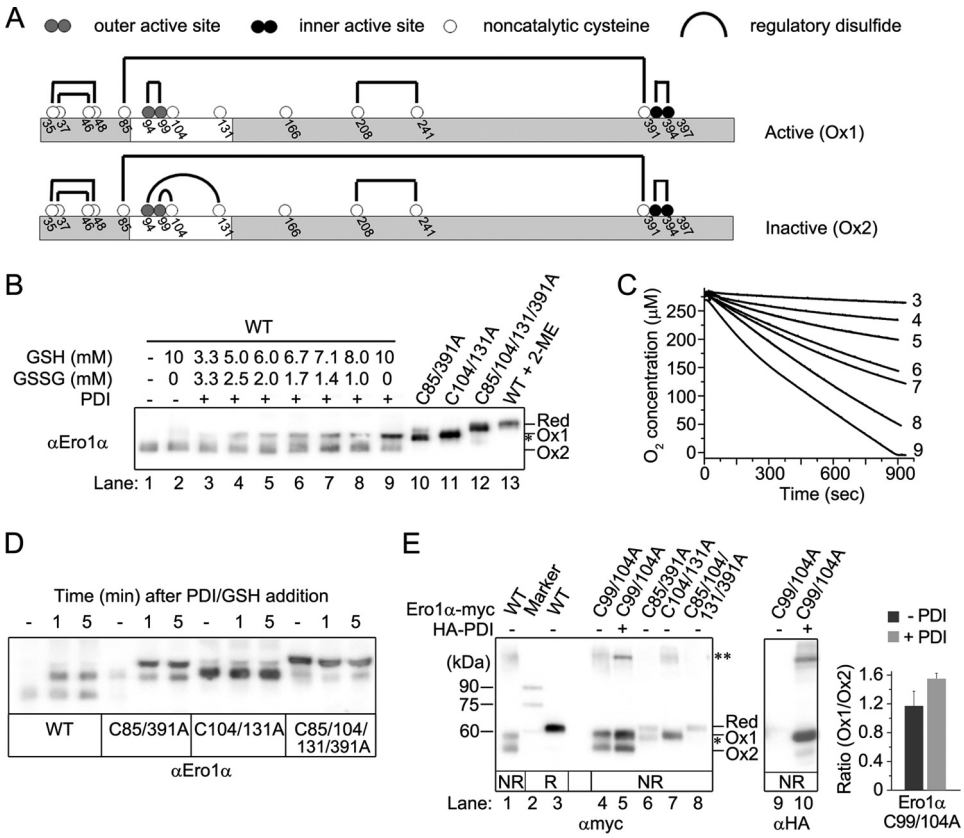

FIGURE 1. **Identification of the regulatory disulfide in Ero1α.** *A*, schematic representation of the disulfide pattern in active (Ox1) and inactive (Ox2) states of Ero1α (7, 14, 23). The cysteine residues are shown as *white*, *gray* (outer active site), and *black* (inner active site) *circles* with numbering, and disulfides are indicated as *lines*. Regulatory disulfides (Cys94-Cys131 and Cys99-Cys104) formed in Ox2 state are indicated by curves (7, 8). Note that the long-range disulfide Cys85-Cys391 is explicitly identified to be a structural but not regulatory disulfide in this work. The flexible loop region is represented by an *open bar*. *B*, Ero1α WT (*lanes 1–9*) of 1 μM was incubated with or without 10 μM PDI in 10 mM glutathione redox buffer composed of various concentrations of GSH and GSSG as indicated at 25 °C for 5 min, then analyzed by nonreducing SDS-9% PAGE and Western blotting (*WB*) with αEro1α. The distinct gel mobilities of three Ero1α Cys-to-Ala mutants (*lanes 10–12*) and fully reduced Ero1α treated with 2-mercaptoethanol (2-ME) (*lane 13*) indicated the reduction of different disulfides. Reduced Ero1α (*Red*), two oxidized Ero1α species (Ox1 without Cys94-Cys131 disulfide and Ox2 with both Cys85-Cys391 and Cys94-Cys131 intact) were indicated. *Asterisk* indicates a species with only Cys85-Cys391 absent (23). *C*, oxygen consumption catalyzed by 2 μM Ero1α WT was monitored in the presence of 20 μM PDI and various concentrations of GSH/GSSG as indicated by numbering the same as in *B*. *D*, 2 μM Ero1α WT and mutants were incubated in the absence (−) or presence of 20 μM PDI and 10 mM GSH for indicated time, analyzed as in *B*. *E*, Myc-tagged Ero1α WT and mutants were co-expressed with (+) or without (−) HA-tagged PDI in HeLa cells. After NEM blocking, cells were lysed and analyzed by nonreducing (*NR*) or reducing (*R*) SDS-8% PAGE, followed by αmyc or αHA WB as indicated. Molecular size markers were shown on the left margin and redox states of Ero1α were indicated as in *B*. *Double asterisks* indicate the Ero1α-PDI complex. The ratios of Ox1/Ox2 of Ero1α C99/104A from *lanes 4* and *5* are shown on the *right panel* (mean ± S.D., $n = 3$).

form in C99/104A as well as pronounced increase of the disulfide-linked Ero1α-PDI heterodimer, but no fully reduced form was observed, indicating that in cells the increase of PDI level promotes the reduction of Cys94-Cys131 but not Cys85-Cys391. Moreover, mutation of Cys85-Cys391 disulfide dramatically impaired the formation of Ero1α-PDI heterodimer, underlining the importance of this bond for maintaining the Ero1α-PDI functional complex. In summary, during the activation of Ero1α the Cys94-Cys131 regulatory disulfide is reduced resulting in the mobility shift from Ox2 to Ox1, whereas the Cys85-Cys391 disulfide remains intact, which is important for the catalytic activity of Ero1α.

Dynamic Regulation of Ero1α Activity in Cells by PDI—To gain further insights into the dynamic regulation of Ero1α during the fluctuation of the ER redox environment in cells, the activation/inactivation processes of Ero1α were studied by monitoring the interconversion between Ox1 and Ox2 forms of the aforementioned Ero1α C99/104A mutant. Firstly, the activation kinetics of Ero1α was examined by stressing the cells with a low concentration of DTT to mimic the burst of free thiols during protein synthesis. Just in 1 min after DTT challenge, a large portion of Ero1α quickly shifted to Ox1 state, but after 10 min there was still a small fraction of Ox2. When PDI was overexpressed, all Ero1α shifted from Ox2 to Ox1 in 1 min (Fig. 2*A*). When cells were pre-treated by a small molecule 16F16, which specifically inhibits the thiol-disulfide oxidoreductase activity of PDI (24), the reduction of Ero1α upon DTT addition was almost completely inhibited, strongly suggesting that PDI plays a critical role in mediating the thiol-driven activation of Ero1α (Fig. 2*B*).

Next, we studied the inactivation process of Ero1α C99/104A by using a DTT pulse-chase assay. In DTT-flooded cells, Ero1α was in Ox1 state with the Cys94-Cys131 regulatory disulfide reduced. At the end of the pulse, Ox2 species quickly re-emerged and increased during the 'chase', but not all Ox1 were re-oxidized to Ox2 after 10 min. Knockdown of PDI significantly delayed the re-emergence of Ero1α Ox2 following the DTT-pulse (Fig. 2*C*). Moreover, when cells were pre-treated with 16F16, the delay of Ero1α inactivation became more conspicuous (Fig. 2*D*), emphasizing the role of redox active PDI in

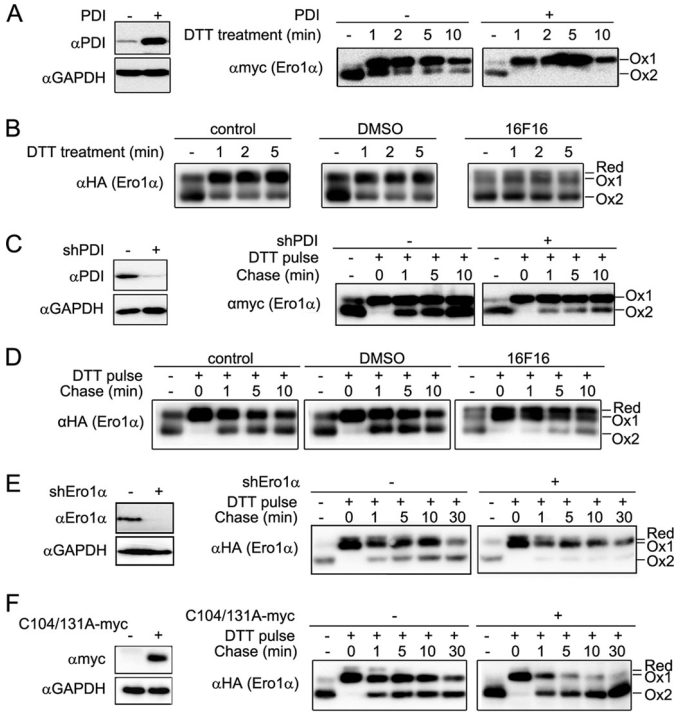

FIGURE 2. **Dynamic regulation of Ero1α by redox active PDI in cells.** *A*, HeLa transfectants expressing Ero1α C99/104A-myc were co-transfected with PDI WT (+) or empty (−) plasmid. *Left panel*, the expression level of PDI was visualized by αPDI WB. *Right panel*, HeLa cells were exposed to 150 μM DTT, aliquots were taken at indicated times and analyzed by nonreducing SDS-9% PAGE and αmyc WB. *B*, to maximally block the active sites of PDI, HeLa transfectants expressing Ero1α C99/104A-HA were treated by 50 μM DTT and 50 μM 16F16 dissolved in DMSO for 8 h before harvest. Parallel treatments by 50 μM DTT alone (control) or combined with DMSO were also carried out. The shift of part of Ero1α to Ox1 at steady state was due to the pre-treatment by 50 μM DTT. The activation of Ero1α was monitored as in *A* and visualized by αHA. *C*, HeLa cells were treated with control (−) or shPDI (+) plasmid and then co-transfected with Ero1α C99/104A-myc. *Left panel*, the knockdown efficiency of PDI is shown by αPDI WB. *Right panel*, after a 10 mM DTT pulse treatment, cells were washed to remove DTT and followed by a chase at indicated times. Cell lysates were analyzed by nonreducing SDS-9% PAGE and αmyc WB. *D*, HeLa transfectants expressing Ero1α C99/104A-HA were treated as in *B*, and the inactivation of Ero1α was monitored as in *C* and visualized by αHA. *E*, *left panel*, expression level of endogenous Ero1α in HeLa cells transfected with control (−) or shEro1α (+) plasmid was monitored by WB using αEro1α. *Right panel*, HeLa cells were treated with control (−) or shEro1α (+) plasmid and then co-transfected with Ero1α C99/104A-HA, which has an altered codon bias to the endogenous *ERO1* gene and is not targeted by the shEro1α. The redox states of Ero1α C99/104A-HA during the pulse-chase process were monitored as in *C* and visualized by αHA. *F*, HeLa transfectants expressing Ero1α C99/104A-HA were co-transfected with the hyperactive Ero1α C104/131A-myc (+) or empty (−) plasmid. *Left panel*, the expression of Ero1α C104/131A-myc was visualized by αmyc WB. *Right panel*, the redox states of Ero1α C99/104A-HA during the pulse-chase process were monitored as in *C* and visualized by αHA. The Red, Ox1, and Ox2 species of Ero1α were indicated on the right margin of each panel.

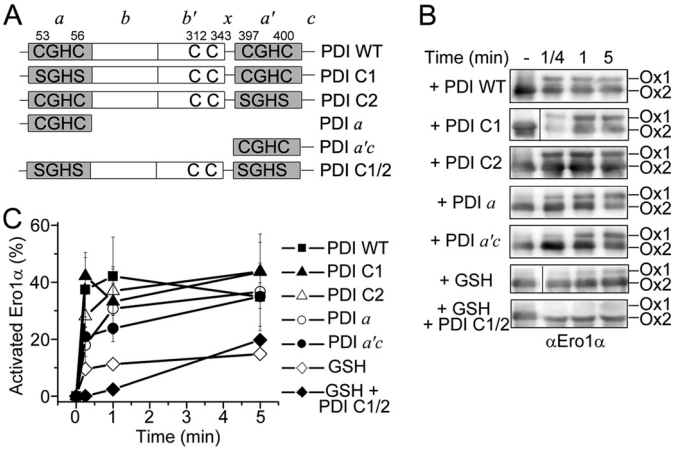

FIGURE 3. **Activation of Ero1α by PDI *in vitro*.** *A*, PDI is composed of four Trx-domains of *a*, *b*, *b′* and *a′*, as well as an *x*-linker and a *c*-tail. Cysteine residues are shown with amino acid numbering, and the -CGHC- active sites and the mutated -SGHS- sites are indicated. *B*, oxidized Ero1α C99/104/166A of 1 μM was mixed with 10 μM reduced PDI or its mutants as indicated. Aliquots were taken at indicated times and analyzed by nonreducing SDS-9% PAGE and αEro1α WB. The vertical line delineates the boundary of juxtaposed lanes which were non-adjacent on the same blot. *C*, percentage of Ox1 species in each lane in *B* was quantified by densitometry and plotted to compare the effects on the activation of Ero1α by PDI proteins (mean ± S.D., $n = 3$).

Ero1α inactivation. As the recovery of ER redox homeostasis (25) and PDI redox balance (26) from a reductive challenge both largely depend on Ero1α oxidase activity, we next looked into whether modulating Ero1α level can affect the inactivation of Ero1α itself. Silencing endogenous Ero1α dramatically inhibited the recovery of Ox2 in Ero1α C99/104A (Fig. 2*E*). Conversely, co-expression of the hyperactive Ero1α C104/131A markedly accelerated the transition from Ox1 to Ox2 in Ero1α C99/104A and reset the redox poise eventually at 30 min (Fig. 2*F*). Taken together, in cells Ero1α is very sensitive to the fluctuation of thiol-disulfide redox states in the ER, and the regulatory disulfides of Ero1α can be modulated by the redox active PDI.

The Two Catalytic Domains of PDI Can Activate Ero1α Independently—PDI contains two -CGHC- active sites respectively located in domain *a* and *a′*. To understand the contribution of the two catalytic domains to the activation of Ero1α, five PDI mutants were prepared (Fig. 3*A*). We tested the *in vitro* ability of these PDI proteins at reduced form to reduce the Cys94-Cys131 regulatory disulfide in Ero1α C99/104/166A mutant. The mutation of the unpaired Cys166 to Ala on the background of C99/104A was to avoid aberrant formation of homodimer during the preparation of homogenous oxidized Ero1α monomer (14). Addition of 10-fold reduced PDI WT to oxidized Ero1α resulted in rapid appearance of Ox1 form within 15 s, but up to 5 min there was still Ox2 remained (Fig. 3*B*), as the reduction potential of the Cys94-Cys131 regulatory disulfide is much lower than that of PDI as mentioned above. PDI C1 or PDI C2, in which both cysteines were replaced by serines in the active site of domain *a* or *a′*, reduced the Cys94-Cys131 regulatory disulfide as efficiently as PDI WT, indicating that either active site of PDI is sufficient to activate Ero1α. PDI C1/2 with both active sites mutated as a negatively control, had little effect on the reduction of Ero1α even though excess GSH was supplied (Fig. 3, *B* and *C*). The ability of catalytic domains of PDI to activate Ero1α was further assessed by isolated PDI *a* and *a′c* domains. Similar to PDI WT both isolated domains reduced ~40% of the Cys94-Cys131 regulatory disulfide in 5 min, although Ox1 form appeared somewhat slower during the initial stage (Fig. 3, *B* and *C*). The above results clearly demonstrated that PDI can directly modulate the fast transition of Ero1α from Ox2 to Ox1 state, and the two catalytic domains of PDI can independently perform the task of activating Ero1α.

Autonomous and PDI-mediated Inactivation of Ero1α—Next, the inactivation process of Ero1α was dissected to address whether the re-oxidation of the regulatory disulfides in Ero1α

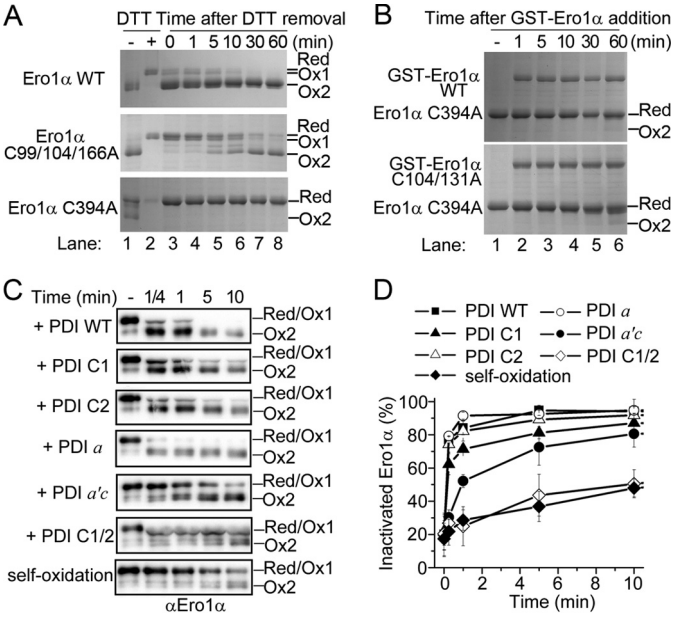

FIGURE 4. **Inactivation of Ero1α *in vitro*.** *A*, redox states of recombinant Ero1α WT and its mutants in the absence (*lane 1*) or presence (*lane 2*) of DTT were shown. After DTT removal, reduced Ero1α and its mutants were diluted to a final concentration of 3 μM to initiate the self-oxidation. Aliquots were taken out at indicated time points (*lanes 3–8*) for analyzes by nonreducing SDS-9% PAGE and Coomassie staining. *B*, 3 μM reduced Ero1α C394 (*lane 1* for alone) was incubated with 3 μM GST-Ero1α WT or GST-Ero1α C104/131A for indicated time points (*lanes 2–6*), and then analyzed as in *A*. *C*, reduced Ero1α C99/104/166A of 1 μM was mixed with 10 μM oxidized PDI or its mutants as indicated. Aliquots were taken at indicated times and analyzed by nonreducing SDS-9% PAGE and αEro1α WB. Note that the Red and Ox1 bands merged together on the blots. *D*, percentage of Ox2 species in each lane in *C* was quantified by densitometry and plotted to compare the effects on the inactivation Ero1α by PDI proteins (mean ± S.D., $n = 3$).

can occur autonomously. Purified Ero1α protein was firstly treated with excess amounts of DTT for full reduction of the regulatory disulfides. After DTT was washed out, most of Ero1α WT immediately converted to the Ox2 form, with only a small portion remained in fully reduced and/or Ox1 form, and a complete conversion to Ox2 form was achieved at 30 min (Fig. 4*A*, *upper panel*). The re-oxidation of Ero1α mutants lacking the outer active site (Ero1α C99/104/166A) or the inner active site (Ero1α C394A) was greatly impaired (Fig. 4*A*, *middle panel*) or completely inhibited (Fig. 4*A*, *lower panel*). Thus, the regulatory disulfides in Ero1α can be autonomously re-oxidized aerobically, and the oxidizing power of oxygen is likely expended by the inner active site (Cys394-Cys397) and transferred via the outer active site (Cys94-Cys99) to re-oxidize the regulatory disulfides. We then examined whether the autonomous re-oxidation of Ero1α is via intramolecular or intermolecular disulfide transfer. To test the latter possibility, reduced Ero1α C394A was incubated with GST-fused Ero1α WT or GST-fused hyperactive Ero1α C104/131A, because they could be clearly separated by distinct molecular weights on SDS-PAGE. As shown in Fig. 4*B*, little oxidized Ero1α C394A was observed up to 60 min after the addition of equimolar active GST-Ero1α proteins, suggesting that the intermolecular disulfide exchange between two Ero1α molecules is not favorable, and the autonomous re-oxidation of Ero1α occurs predominantly via intramolecular disulfide transfer.

The Ero1α C99/104/166A mutant with slow autonomous re-oxidation was used to further study the contribution of PDI to the inactivation dynamics of Ero1α. Consistent with the data in cells that rapid inactivation of Ero1α depends on active PDI (Fig. 2), oxidized PDI WT markedly accelerated the reappearance of Ox2, with ~70% of Ero1α being oxidized to Ox2 state at 15 s and complete oxidation at 5 min (Fig. 4, *C* and *D*). PDI C1 and PDI C2 promoted the re-oxidation of Ero1α as efficiently as PDI WT, suggesting that the two active sites functions also independently in the inactivation of Ero1α. The catalytic inactive mutant PDI C1/2 did not show any effect as expected. Again, the isolated PDI *a* and PDI *a′c* domains accelerated the re-oxidation of Ero1α, albeit PDI *a′c* was less efficient (Fig. 4, *C* and *D*). Taken together, the inactivation process of Ero1α as monitored by the re-oxidation of Cys94-Cys131 regulatory disulfide can be directly promoted by either active site of PDI.

Asymmetric Oxidation of PDI by Ero1α Ensures Efficient Oxidative Folding—The above results showed that the two catalytic domains of PDI contribute to the activation/inactivation of Ero1α equally, whereas we and others previously observed that Ero1α drives substrate oxidation preferentially through the *a′* domain of PDI (8, 12). So we explored the biological significance of asymmetric oxidation of PDI by Ero1α catalytic activity. The gel-based methoxy polyethyleneglycol 5000 maleimide (mPEG-5k) modification assay can monitor the redox state change of PDI (7, 27), and PDI oxidized by Ero1α would have less free cysteines to be modified by mPEG-5k and migrate faster. As shown in Fig. 5*A* after reacting with Ero1α for 30 min, PDI WT was not completely oxidized with significant fully/semi-reduced species remained, PDI C1 was more oxidized, and PDI C2 was barely oxidized. As reduced PDI is required to rearrange the non-native disulfides (2), we speculated that the asymmetric and incomplete oxidation of PDI by Ero1α may be important for PDI to catalyze disulfide isomerization in addition to disulfide formation. To test this hypothesis, reactivation of scrambled RNase A with promiscuous disulfides in the Ero1α/PDI system was used for isomerase activity assay. As shown in Fig. 5*C*, after oxidation by Ero1α the isomerase activities of PDI WT and PDI C1 were compromised, but not completely depleted. Of note, the isomerase activity of PDI C2 was little affected, supporting the idea that the *a* domain of PDI is resistant to Ero1α oxidation and can function as an efficient isomerase. To further examine this rationale, yeast Ero1p/Pdi1p system was studied because the oxidation pattern of the two active sites in Pdi1p catalyzed by Ero1p is different from that in mammalian system (28). Under our experimental conditions Pdi1p was very efficiently oxidized by Ero1p with little fully/semi-reduced Pdi1p left at 30 min, and the oxidation rate of Pdi1p C2 by Ero1p was slightly faster than that of Pdi1p C1 (Fig. 5*B*), which is quite different from the Ero1α/PDI system indeed (Fig. 5*A*). Consequently, the isomerase activities of Pdi1p WT and its active site mutants were fully suppressed upon Ero1p oxidation (Fig. 5*D*).

To gain further insights into the merits of asymmetric oxidation of PDI by Ero1α, we monitored the *de novo* oxidative folding of another classical folding substrate, bovine pancreatic trypsin inhibitor (BPTI). Native BPTI contains three disulfide bonds, and its successful folding depends on the rearrangement

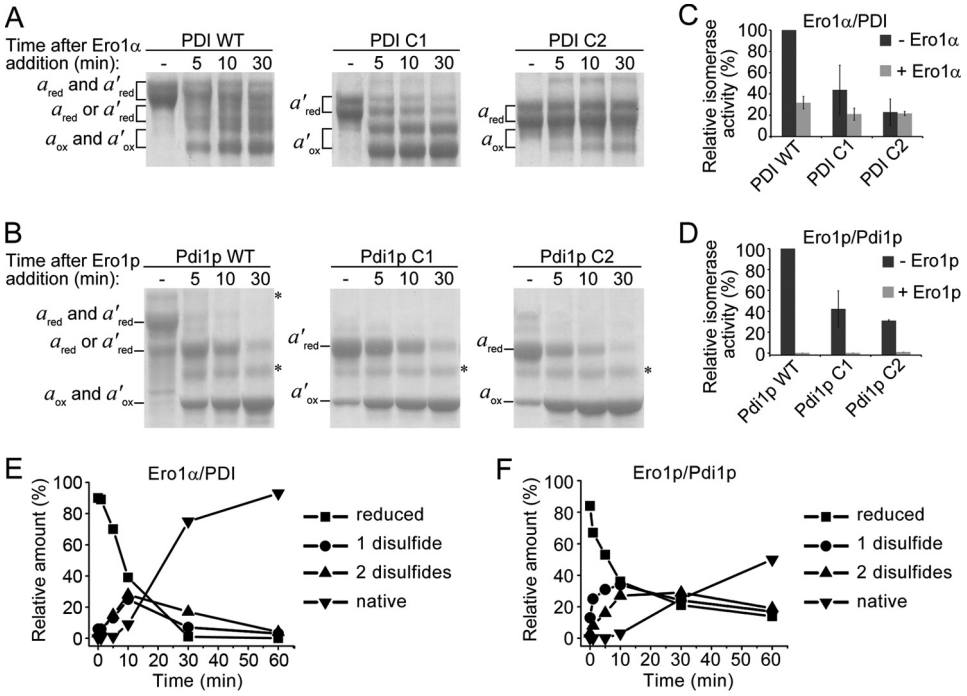

FIGURE 5. **Asymmetric oxidation of PDI by Ero1α endows PDI with both oxidoreductase and isomerase activities.** *A* and *B*, loss of reactivity toward mPEG-5k upon disulfides formation in PDI (*A*) or Pdi1p (*B*) proteins catalyzed by Ero1α or Ero1p, respectively, was monitored by SDS-10% PAGE and visualized by Coomassie staining. a_{red}, a_{ox}, a'_{red}, and a'_{ox} indicate the PDI proteins with *a* domain reduced, *a* domain oxidized, *a′* domain reduced and *a′* domain oxidized, respectively. The doublet bands of each PDI species are resulted from one or both cysteines in domain *b′* being alkylated by mPEG-5k. *Asterisks* in *B* indicate the Pdi1p species with a structural disulfide (Cys90-Cys97) in domain *a* being reduced and modified by mPEG-5k. *C* and *D*, isomerase activities of PDI (*C*) and Pdi1p (*D*) proteins for the reactivation of scrambled RNase A were determined after incubation with or without Ero1 oxidases as indicated (mean ± S.D., $n = 3$). *E* and *F*, oxidative folding of denatured and reduced BPTI was catalyzed by Ero1α/PDI (*E*) or Ero1p/Pdi1p (*F*) and analyzed by reverse-phase HPLC. The percentage of reduced BPTI, one disulfide containing species, two disulfides containing species and native BPTI at 0, 1, 5, 10, 30, and 60 min were quantified. Values were the mean of two independent experiments with very similar profiles.

of the kinetically trapped disulfide intermediates (29). The quantitative dissection of BPTI refolding steps showed that in the first 10 min Ero1α/PDI catalyzed the oxidation of reduced BPTI to various intermediates, which were further oxidized to native BPTI at 60 min with the yield over 90% (Fig. 5*E*). In Ero1p/Pdi1p system, although the oxidation of reduced BPTI in the first 10 min was slightly faster than that in Ero1α/PDI system, the one-disulfide and two-disulfide species remained in later steps and only ~50% BPTI was refolded to native state after 60 min (Fig. 5*F*). Thus, human Ero1α/PDI system is more efficient than yeast Ero1p/Pdi1p system in proofreading non-native disulfides. In conclusion, the asymmetry in Ero1α catalyzed oxidation of PDI is functionally significant, which makes the *a′* domain act primarily as an oxidase and the *a* domain act as an isomerase so as to ensure efficient oxidative folding of client proteins.

Role of Hydrophobic Interaction in Ero1α-PDI Interplay—We further explored the mechanisms underlying the intriguing phenomenon that both catalytic domains of PDI can react with the regulatory disulfides of Ero1α without discrimination but only the *a′* domain can mediate efficient electron transfer to the outer active site of Ero1α. We and others previously found that the principle substrate binding domain *b′* in PDI is critical for the Ero1α/PDI disulfide relay (12, 14), therefore we studied whether the substrate binding ability of PDI is also required for the activation/inactivation of Ero1α. Here we took the advantage of the mutation of two residues Phe-275 and Ile- 289 in the *b′* domain of PDI, which dramatically eliminates binding with peptide or Ero1α (10, 30). Surprisingly, PDI binding mutant F275W/I289A at reduced form was able to reduce the Cys94-Cys131 regulatory disulfide in Ero1α as efficiently as PDI WT (Fig. 6*A*), and the oxidized binding mutant also facilitated the re-oxidation of Ero1α (Fig. 6*B*). Thus, the peptide binding ability of PDI *b′* domain is not required in the reduction/oxidation of the regulatory disulfides in Ero1α.

To explore which form of Ero1α binds with PDI, HA-tagged PDI WT was further used to co-immunoprecipitate Ero1α in HeLa cells. Only Ox1 but not Ox2 species of Ero1α was detected with PDI under nonreducing conditions (Fig. 6*C*), indicating that PDI specifically recognizes the active form of Ero1α through non-covalent interaction. A surfactant Triton X-100 and a hydrophobic probe 1-anilinonaphthalene-8-sulfonate (ANS) both markedly inhibited the oxygen consumption by active Ero1α during the oxidation of PDI (Fig. 6, *D* and *E*), emphasizing the functional role of hydrophobic binding in Ero1α and PDI disulfide relay. Interestingly, Triton X-100 and ANS only slightly affected Ero1p/Pdi1p activity (Fig. 6, *D* and *E*), implying that the hydrophobic interaction between Ero1α and PDI is a critical requirement for mammals. Gel filtration chromatography of mixed PDI and Ero1α showed a new peak fraction with the molecular weight larger than that of the separated proteins (Fig. 6*F*), confirming the presence of a stable complex between PDI and Ero1α. The majority of this complex was formed via non-covalent interaction and the minority was linked by intermolecular disulfide bridges (Fig. 6*F*). In line with activity assays, negligible complex of Ero1p and Pdi1p was

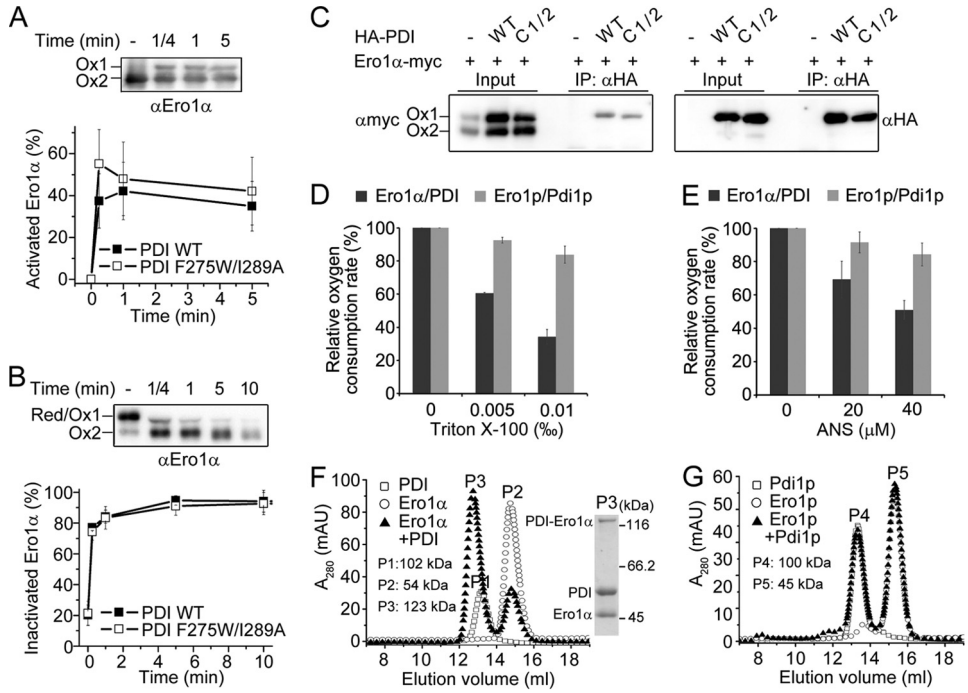

FIGURE 6. **Role of hydrophobic interaction in Ero1α/PDI interplay.** *A* and *B*, activation (*A*) and inactivation (*B*) of 1 μM Ero1α C99/104/166A by 10 μM PDI F275W/I289A were monitored as in Figs. 3*B* and 4*C*, respectively. The percentage of Ox1 species in *A* or Ox2 species in *B* was quantified by densitometry, compared with the PDI WT plots in Figs. 3*C* or 4*D*, respectively (mean ± S.D., $n = 3$). *C*, lysates from HeLa transfectants expressing Ero1α-myc without or with HA-PDI as indicated were analyzed directly by nonreducing SDS-8% PAGE and WB (*Input*) or after immunoprecipitation (*IP*) with αHA. *D* and *E*, oxidation of 20 μM PDI or Pdi1p, respectively, by 2 μM hyperactive Ero1α C104/131A or Ero1p C150/295A was determined by monitoring the rate of oxygen consumption in the presence of 10 mM GSH and various concentrations of Triton X-100 (*D*) or ANS (*E*) as indicated. The oxygen consumption rate was calculated from the slope of the linear phase of oxygen decrease, and the rates obtained in the absence of Triton X-100 or ANS were taken as 100% (mean ± S.D., $n = 3$). *F* and *G*, human (*F*) or yeast (*G*) PDI and Ero1 proteins, as well as their mixtures after a 30 min pre-incubation at a molar ratio of 1:1.3 were analyzed by a Superdex 200 10/300 GL column under room temperature at a flow rate of 0.5 ml/min. Apparent molecular weight of each peak as shown was calculated using protein standards: blue dextran (2000 kDa), albumin (67 kDa), ovalbumin (43 kDa), chymotrypsinogen (25 kDa), and RNase A (13.7 kDa). P3 fraction in *F* was collected, quenched by NEM, and then analyzed by nonreducing SDS-10% PAGE and visualized by Coomassie staining.

detected on gel filtration (Fig. 6*G*). Collectively, all the above data support our model that modulation of the regulatory disulfides in Ero1α by both PDI active sites is independent from the *b*′ domain, while the hydrophobic interaction is necessary for the catalytic oxidation of PDI *a*′ domain by active Ero1α. In contrast, there is no stable hydrophobic binding between yeast Ero1p and Pdi1p, and both active sites of Pdi1p can freely react with the regulatory disulfides (31) as well as the catalytic disulfide ((28) and Fig. 5*B*) in Ero1p due to less conformational restriction.

Interplay between Ero1α and Other PDIs—It is known that Ero1α and its hyperactive homologue Ero1β poorly catalyze the oxidation of other PDI family members (9, 15), but transient mixed-disulfides between Ero1α and several PDIs were trapped in cells (32, 33). We speculated these intermediates might be formed during the reduction/oxidation of the regulatory disulfides in Ero1α by PDIs. Therefore PDIp, P5, ERp46, ERp57, and ERp72 were overexpressed in HeLa cells to check whether they were able to function as regulators of Ero1α. Overexpression of these PDIs to a similar level had only moderate effects on the Ox1/Ox2 ratio of Ero1α at steady state compared with PDI (Fig. 7*A*, *first lane in upper panel*). However, when the cells were treated with a low concentration of DTT, these oxidoreductases except ERp72 rapidly promoted the reduction of Ero1α (Fig. 7*A*), underscoring their roles in facilitating Ero1α activation against reductive challenge in the ER. Thus, the inefficient functional oxidation of other PDIs by Ero1α may not be attributed to poor Ero1α activation. As the substrate binding domain *b*′ in PDI plays a critical role in enzymatic disulfide relay between PDI and Ero1α, we realized that lack of the unique *b*′ domain of PDI in other PDIs could be a reason for their inefficient oxidation by Ero1α. To test this possibility, chimeric PDI-PDIs proteins were constructed by fusing one catalytic domain from each of the five PDIs to the C terminus of the rigid *bb*′ base of PDI. The rates of Ero1α catalyzed oxygen consumption were dramatically increased in the presence of the chimeras PDI-PDIp, PDI-ERp57 and PDI-ERp72 (Fig. 7*B*). PDI-ERp46 only modestly increased the reaction rate and PDI-P5 was not effective (Fig. 7*C*). As the catalytic domains from PDIp, ERp57, and ERp72 used to generate the chimeras are *a*′-type while those from ERp46 and P5 are *a*-type, these results explained why other PDIs are poor substrates of Ero1α, and strengthened the molecular mechanism we proposed that both the *b*′ and *a*′ domains are necessary for the functional disulfide relay between Ero1α and PDI (12). As expected, all the PDIs and PDI-PDIs chimeras efficiently promoted the transition of Ero1α from Ox2 to Ox1 state during Ero1α catalyzed reactions (Fig. 7*D*), indicating that all PDIs tested are capable to activate Ero1α *in vitro*.

Next, the abilities of PDIs to inactivate Ero1α were studied by using the reconstituted system. PDIp, P5, ERp46 and ERp57 re-oxidized reduced Ero1α as efficient as PDI, and ERp72

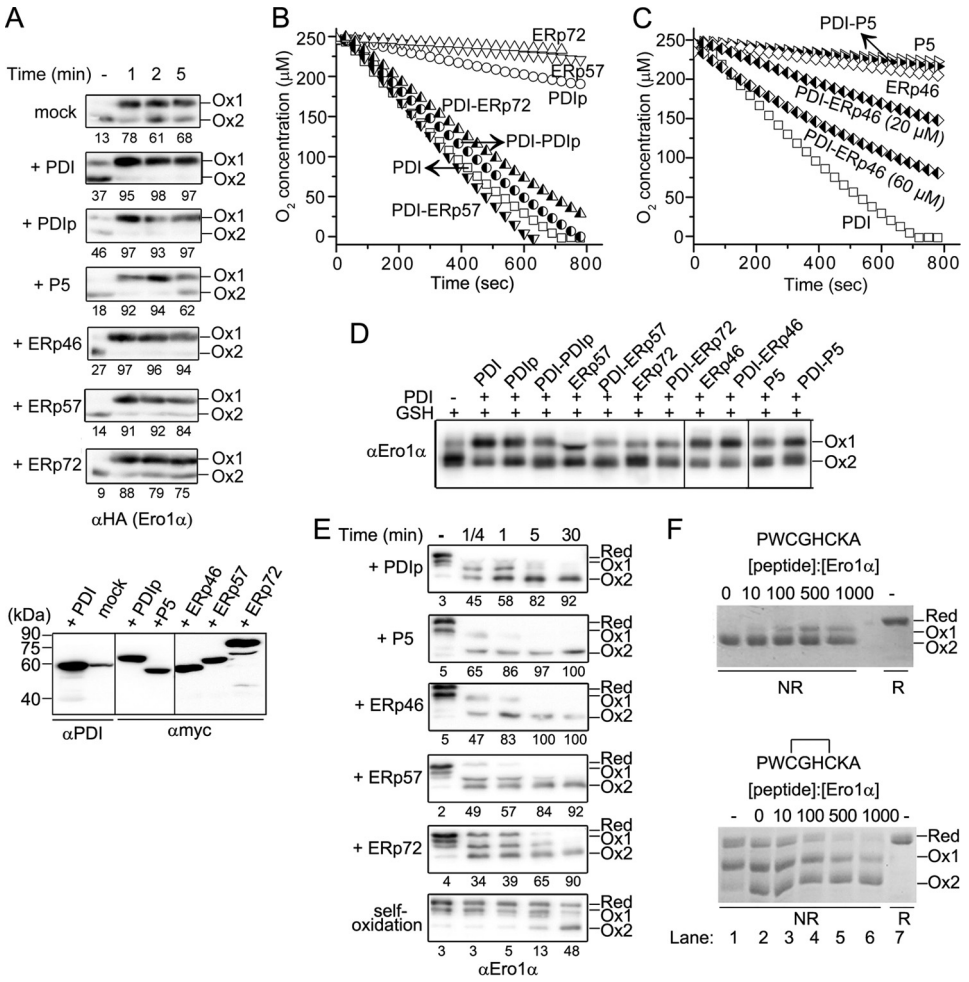

FIGURE 7. **Several PDI family proteins are potent regulators but poor substrates of Ero1α.** *A*, HeLa transfectants expressing Ero1α C99/104A-HA were co-transfected with mock or PDIs plasmid as indicated. *Upper panel*, the activation of Ero1α was carried out as in Fig. 2*A*, and visualized by αHA WB. The percentage of Ox1 species in each lane was quantified by densitometry and indicated below. *Lower panel*, cell lysates were also analyzed by reducing gel and WB, with αPDI and αmyc to visualize PDI and other PDIs, respectively. *B* and *C*, oxygen consumption by 2 μM Ero1α WT during oxidation of 20 μM PDIs and PDI-PDIs chimeras was monitored in the presence of 10 mM GSH. PDI-ERp46 at 60 μM was also used. *D*, in parallel experiments to *B* and *C*, aliquots were taken at 5 min after the initiation of the reaction, quenched by NEM and analyzed by nonreducing SDS-9% PAGE and αEro1α WB. *E*, inactivation of 1 μM reduced Ero1α C99/104/166A by 10 μM oxidized PDIs was performed as in Fig. 4*C* and visualized by αEro1α WB. The percentage of Ox2 species in each lane was quantified by densitometry and indicated below. *F*, potency of the -CGHC- active site containing motif (PWCGHCKA) of PDI for regulation of Ero1α. *Upper panel*, 2 μM oxidized Ero1α WT was incubated with reduced octapeptide at excess fold to Ero1α as indicated for 5 min. *Lower panel*, 2 μM freshly prepared reduced Ero1α C99/104/166A (*lane 1*) was incubated with oxidized octapeptide (*lanes 2–6*) for 5 min. After NEM blocking, the samples were analyzed by nonreducing (*NR*) SDS-9% PAGE and visualized by Coomassie staining. Reducing (*R*) Ero1α samples were also loaded for comparison.

showed somewhat weaker effects in terms of the disappearance of fully reduced Ero1α (Fig. 7*E*). We were then interested in whether the -CGHC- active site containing motif, which is conserved among these PDIs, is sufficient to reduce/oxidize the regulatory disulfides in Ero1α. A synthesized octapeptide (PWCGHCKA) derived from PDI in its reduced form indeed promoted the activation of Ero1α in a dose dependent manner, and the oxidized octapeptide facilitated the inactivation of Ero1α in a similar way (Fig. 7*F*), suggesting that the -CGHC- active site is the minimal element for regulation of Ero1α. The high-dose of octapeptide used here implied that the intact catalytic Trx domain is optimized for efficient reduction/oxidation of Ero1α. Altogether, the above data strongly suggested that PDIs with catalytic domain containing the -CGHC- active sites, if not all, are potent regulators of Ero1α. However, active Ero1α can only efficiently catalyze disulfide production via PDI due to the specific recognition of PDI *b′-a′* domains.

DISCUSSION

Ero1α activity is tightly regulated in mammalian ER by a feedback mechanism. At resting state of cells, formation of the two regulatory disulfides (Cys94-Cys131 and Cys99-Cys104) in Ero1α restricts the availability of the Cys94-Cys99 outer active site (7, 23). The inactive Ero1α must be promptly activated once robust protein oxidative folding capacity is required, and the activated Ero1α must be adequately inactivated to prevent over-oxidation within the ER. Here, we demonstrate that both the activation and inactivation of Ero1α by PDI *in vitro* occur very fast (<15 s). Similarly, when cells suffer or recover from a reductive challenge the reduction/oxidation of the regulatory disulfides in Ero1α happens rapidly within 1 min. Therefore, the interconversion between inactivated and activated Ero1α responding to the ER redox environment is prompt. Interestingly, we also find that after reductive challenge substantial oxi-

dase activity of Ero1α is required to re-establish the thiol-disulfide balance in the ER on a relative longer time-scale. Previous studies have shown that after reductive challenge the resetting of the steady-state ratio of GSSG to total glutathione is very fast on a time-scale of seconds (25), but the re-oxidation of disulfides in protein substrates takes longer time to be completed (34, 35). Thus, we propose when cells encounter a reductive challenge Ero1α is quickly activated by reduced PDI to catalyze the oxidation of GSH by cooperating with PDI, which results in fast reset of GSH/GSSG balance within 1 min, and Ero1α is then partly inactivated. The remaining active Ero1α drives the oxidation of protein substrates until the thiol-disulfide status in the ER reaches rebalance. After that, Ero1α is inactivated by oxidized PDI to prevent futile consumption of GSH and excessive peroxide production.

Previously, it was reported that several other PDIs (including ERp46, ERp57, ERp72, and P5) can hardly modulate the redox states of Ero1α at steady state, although their redox equilibrium constants with glutathione are close to that of PDI (15). By real-time monitoring the redox states of Ero1α, we clearly show that the activation of Ero1α upon reductive challenge is indeed significantly promoted when PDI, PDIp, P5, ERp46, or ERp57 was individually overexpressed in cells, and these PDIs at oxidized form can accelerate the inactivation of Ero1α *in vitro* (Fig. 7). One exception with unknown reasons is ERp72, which seems less efficient than the other PDIs to regulate Ero1α. Our new finding that many PDIs are potent regulators of Ero1α leads us to propose that the redox state of Ero1α is controlled by the redox balance of PDIs ensemble in the ER (Fig. 8). Since PDIs have substrate specificity in different tissue or cell types, the oxidase activity of Ero1α can thus be precisely regulated in cells with distinct proteomes. Recently, studies have reported the redox regulation of the different unfolded protein response (UPR) sensors was mediated by specific PDIs (36). Therefore, a redox-based feedback regulation loop for controlling the strength of UPR signaling likely exists in the ER, that fine-tuning Ero1α activity by PDIs maintains ER redox homeostasis, which will in turn keep balance of the redox states of PDIs and promote the adaptive UPR as well as attenuate the fatal UPR to avoid cell death.

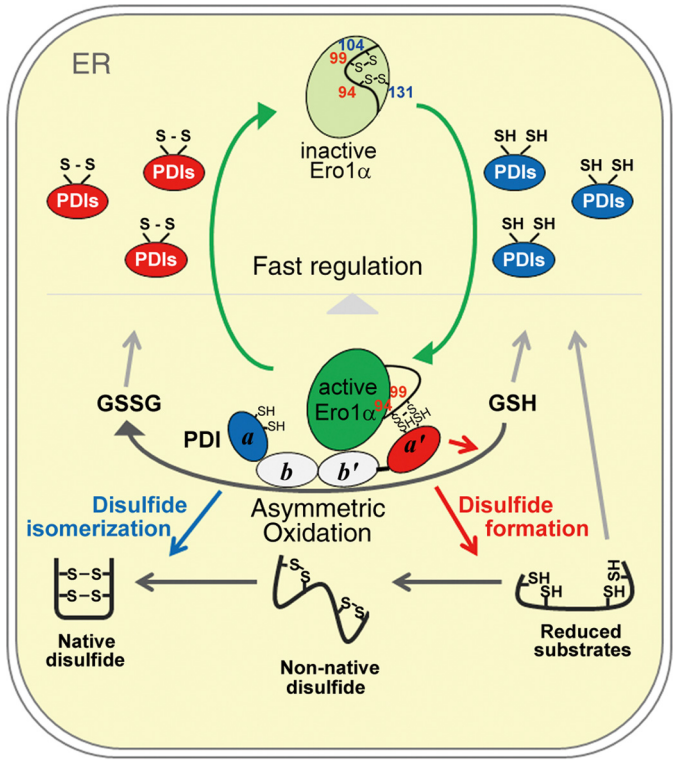

FIGURE 8. **Model for efficient oxidative protein folding in mammalian ER functioned by interplay between Ero1α and PDIs.** At steady states, Ero1α in the ER lumen is predominantly in the inactive states, and PDIs oxidoreductases are present in a balanced reduced (*blue*) and oxidized (*red*) distribution (only the catalytic domain is shown for simplicity). Once the loading of reduced nascent substrates explodes, the redox homeostasis in the ER will be disturbed, and reduced substrates as well as increased GSH generate more reduced PDIs. These reduced PDIs quickly reduce the regulatory disulfides (Cys94-Cys131 and Cys99-Cys104) of Ero1α, and liberate the outer active site located in the loop region (*green arrow*, right). The activated Ero1α specifically recognizes the *b′-a′* domains of PDI and preferentially oxidizes the active site in the *a′* domain, which further introduces disulfides into reduced substrates and GSH (*red arrows*). The asymmetric oxidation of PDI by Ero1α keeps the *a* domain in reduced state, which functions to catalyze efficient disulfide isomerization for the production of correctly folded substrates with complicated disulfides (*blue arrow*). Once the thiol-disulfide equilibrium in the ER is reestablished, the regulatory disulfides of Ero1α are easily re-formed either by self-oxidation or facilitated by oxidized PDIs to decrease the flow of oxidizing power into ER and avoid the futile oxidation cycles (*green arrow*, left).

In this report, we find that the reduction/oxidation of the regulatory disulfides in Ero1α relies on the catalytic activity of PDI but is independent from the peptide binding activity of PDI, and either active site of PDI can facilitate the regulation of Ero1α independently. This novel mode for PDI-mediated regulation of Ero1α is supported by several evidences: 1) single catalytic domain *a* or *a′* of PDI functions well to promote the reduction/oxidation of the regulatory disulfides of Ero1α; 2) an octapeptide containing the -CGHC- active site of PDI alone is capable of regulating Ero1α; 3) the activation and inactivation of Ero1α in cells are dramatically abolished by a PDI inhibitor 16F16, which modifies the active sites of PDI; 4) the substrate binding deficient mutant PDI F275W/I289A regulates Ero1α as efficiently as PDI WT. This mode also well explains why other PDIs containing the -CGHC- active site are also potent regulators of Ero1α, even though they lack the unique *b′* domain of PDI. During preparation of this paper we noticed a very recent study claiming that the substrate binding ability of PDI is crucial for the inactivation of Ero1α, according to the observation that a binding mutant PDI I272A/D346A/D348A (residue numbered without the 17-residue signal sequence) was not able to inactivate Ero1α under anaerobic conditions (37). This triple mutant was originally screened out for stabilization of the *b′x* fragment of PDI in a capped conformation (38), but in full-length PDI the existence of the neighboring *a′* domain limits the *x*-linker to be in a fully capped conformation (39). Thus, the inefficiency of the I272A/D346A/D348A mutant to inactivate Ero1α in their experiments may not be properly attributed to the loss of peptide binding activity.

Once being activated, the reduction of the regulatory disulfides probably increases the conformational flexibility of the regulatory loop between Cys-94 and Cys-131 (14), so that Ero1α can specifically bind to PDI via hydrophobic interactions (Fig. 6), like an unfolded nascent peptide being captured by the substrate binding site of PDI. By recognizing the *b′-a′* fragment of PDI, Ero1α specifically catalyzes the oxidation of the active

site in the *a′* domain of PDI. Other PDIs are poor substrates of Ero1α and cannot increase the ratio of activated/inactivated Ero1α at steady state because they cannot bind and stabilize the active form of Ero1α due to the lack of the peptide binding domain *b′* in PDI. Intriguingly, if the *a′*-type domain of PDIp, ERp57 or ERp72 is fused to the *bb′* base of PDI, the chimera becomes competent substrate for Ero1α oxidase activity. The two different interaction modes between Ero1α and PDIs described above ensures that the activity of Ero1α can be elegantly regulated by sensing the redox states of the PDIs ensemble, while Ero1α specifically produces disulfides through the *a′* domain of PDI, so that the ER is protected from over-oxidation caused by promiscuous oxidation of PDI *a* domain and other PDIs.

The biological implication of the strong preference on the *a′* domain by Ero1α oxidase activity has been revealed in this study. In the Ero1α-driven oxidative folding, PDI *a′* domain acts primarily as an oxidase to transfer disulfides into folding substrate, while PDI *a* domain acts as an efficient isomerase to proofread incorrect disulfides. Under physiological conditions the semioxidized state of PDI is important for the efficiency and fidelity of oxidative protein folding (Fig. 8). Distinct from the mammalian system, there is little stable hydrophobic binding between yeast Ero1p and Pdi1p, which makes less conformational restriction for active Ero1p to transfer disulfides into either catalytic domain of Pdi1p. The strong oxidation of Pdi1p by Ero1p favors fast disulfide generation but compromises the isomerase activity required for catalyzing native disulfide formation (Fig. 5). Our results are in line with the observation that Pdi1p oxidase activity is critical to yeast growth and viability and less than 6% of its isomerase activity is needed (40). Actually, Pdi1p exists predominantly in oxidized state in yeast cells (27), whereas a majority of the active sites of PDI in human cells is in reduced state (41). It is known that only ~1% proteins (78 in 6,623 total proteins) in *Saccharomyces cerevisiae* are predicted to contain disulfides, much smaller than the percentage of ~16% (3,297 in 20,258 total proteins) in human (www.uniprot.org). Therefore, the less demand of isomerase activity in yeast than in mammals appears reasonable, and the Ero1α/PDI system in mammals has evolved to adapt to the folding of larger and more complicated disulfide proteome.

Acknowledgments—We thank Roberto Sitia, Lloyd Ruddock, Yi Yang, and Xi Wang for their generous gifts of constructs and reagents, Lili Niu (Laboratory of Proteomics, Institute of Biophysics) for technical assistance in HPLC analysis, and the laboratory members for helpful discussions.

REFERENCES

1. Bulleid, N. J., and Ellgaard, L. (2011) Multiple ways to make disulfides. *Trends Biochem. Sci.* **36,** 485–492
2. Hatahet, F., and Ruddock, L. W. (2009) Protein disulfide isomerase: a critical evaluation of its function in disulfide bond formation. *Antioxid. Redox. Signal.* **11,** 2807–2850
3. Sevier, C. S., and Kaiser, C. A. (2008) Ero1 and redox homeostasis in the endoplasmic reticulum. *Biochim. Biophys. Acta* **1783,** 549–556
4. Araki, K., and Inaba, K. (2012) Structure, mechanism, and evolution of Ero1 family enzymes. *Antioxid. Redox. Signal.* **16,** 790–799
5. Cabibbo, A., Pagani, M., Fabbri, M., Rocchi, M., Farmery, M. R., Bulleid, N. J., and Sitia, R. (2000) ERO1-L, a human protein that favors disulfide bond formation in the endoplasmic reticulum. *J. Biol. Chem.* **275,** 4827–4833
6. Pagani, M., Fabbri, M., Benedetti, C., Fassio, A., Pilati, S., Bulleid, N. J., Cabibbo, A., and Sitia, R. (2000) Endoplasmic reticulum oxidoreductin 1-lbeta (ERO1-Lβ), a human gene induced in the course of the unfolded protein response. *J. Biol. Chem.* **275,** 23685–23692
7. Appenzeller-Herzog, C., Riemer, J., Christensen, B., Sørensen, E. S., and Ellgaard, L. (2008) A novel disulphide switch mechanism in Ero1α balances ER oxidation in human cells. *EMBO J.* **27,** 2977–2987
8. Baker, K. M., Chakravarthi, S., Langton, K. P., Sheppard, A. M., Lu, H., and Bulleid, N. J. (2008) Low reduction potential of Ero1α regulatory disulphides ensures tight control of substrate oxidation. *EMBO J.* **27,** 2988–2997
9. Wang, L., Zhu, L., and Wang, C. C. (2011) The endoplasmic reticulum sulfhydryl oxidase Ero1beta drives efficient oxidative protein folding with loose regulation. *Biochem. J.* **434,** 113–121
10. Araki, K., and Nagata, K. (2011) Functional in vitro analysis of the ERO1 protein and protein-disulfide isomerase pathway. *J. Biol. Chem.* **286,** 32705–32712
11. Otsu, M., Bertoli, G., Fagioli, C., Guerini-Rocco, E., Nerini-Molteni, S., Ruffato, E., and Sitia, R. (2006) Dynamic retention of Ero1α and Ero1β in the endoplasmic reticulum by interactions with PDI and ERp44. *Antioxid. Redox. Signal.* **8,** 274–282
12. Wang, L., Li, S. J., Sidhu, A., Zhu, L., Liang, Y., Freedman, R. B., and Wang, C. C. (2009) Reconstitution of human Ero1-Lα/protein-disulfide isomerase oxidative folding pathway in vitro. Position-dependent differences in role between the a and a′ domains of protein-disulfide isomerase. *J. Biol. Chem.* **284,** 199–206
13. Chambers, J. E., Tavender, T. J., Oka, O. B., Warwood, S., Knight, D., and Bulleid, N. J. (2010) The reduction potential of the active site disulfides of human protein disulfide isomerase limits oxidation of the enzyme by Ero1α. *J. Biol. Chem.* **285,** 29200–29207
14. Inaba, K., Masui, S., Iida, H., Vavassori, S., Sitia, R., and Suzuki, M. (2010) Crystal structures of human Ero1α reveal the mechanisms of regulated and targeted oxidation of PDI. *EMBO J.* **29,** 3330–3343
15. Araki, K., Iemura, S., Kamiya, Y., Ron, D., Kato, K., Natsume, T., and Nagata, K. (2013) Ero1-α and PDIs constitute a hierarchical electron transfer network of endoplasmic reticulum oxidoreductases. *J. Cell Biol.* **202,** 861–874
16. Cheng, H., Wang, L., and Wang, C. C. (2010) Domain a′ of protein disulfide isomerase plays key role in inhibiting α-synuclein fibril formation. *Cell Stress Chaperone* **15,** 415–421
17. Wang, L., Zhang, L., Niu, Y., Sitia, R., and Wang, C. C. (2014) Glutathione peroxidase 7 utilizes hydrogen peroxide generated by Ero1α to promote oxidative protein folding. *Antioxid. Redox Signal.* **20,** 545–556
18. Chu, Y. Y., Yang, C., Chen, X. J., Zheng, W. Y., Yang, Y., and Tang, Y. (2009) Structure-function analysis of human protein Ero1-Lα. *Biochem. Biophys. Res. Commun.* **389,** 645–650
19. Li, S. J., Hong, X. G., Shi, Y. Y., Li, H., and Wang, C. C. (2006) Annular arrangement and collaborative actions of four domains of protein-disulfide isomerase: a small angle X-ray scattering study in solution. *J. Biol. Chem.* **281,** 6581–6588
20. Ou, W., and Silver, J. (2006) Role of protein disulfide isomerase and other thiol-reactive proteins in HIV-1 envelope protein-mediated fusion. *Virology* **350,** 406–417
21. Hillson, D. A., Lambert, N., and Freedman, R. B. (1984) Formation and isomerization of disulfide bonds in proteins: protein disulfide-isomerase. *Methods Enzymol.* **107,** 281–294
22. Lyles, M. M., and Gilbert, H. F. (1991) Catalysis of the oxidative folding of ribonuclease A by protein disulfide isomerase: dependence of the rate on the composition of the redox buffer. *Biochemistry* **30,** 613–619
23. Hansen, H. G., Schmidt, J. D., Søltoft, C. L., Ramming, T., Geertz-Hansen, H. M., Christensen, B., Sørensen, E. S., Juncker, A. S., Appenzeller-Herzog, C., and Ellgaard, L. (2012) Hyperactivity of the Ero1α oxidase elicits endoplasmic reticulum stress but no broad antioxidant response. *J. Biol. Chem.* **287,** 39513–39523
24. Hoffstrom, B. G., Kaplan, A., Letso, R., Schmid, R. S., Turmel, G. J., Lo, D. C., and Stockwell, B. R. (2010) Inhibitors of protein disulfide isomerase

suppress apoptosis induced by misfolded proteins. *Nat. Chem. Biol.* **6,** 900–906
25. Appenzeller-Herzog, C., Riemer, J., Zito, E., Chin, K. T., Ron, D., Spiess, M., and Ellgaard, L. (2010) Disulphide production by Ero1α-PDI relay is rapid and effectively regulated. *EMBO J.* **29,** 3318–3329
26. Chin, K. T., Kang, G., Qu, J., Gardner, L. B., Coetzee, W. A., Zito, E., Fishman, G. I., and Ron, D. (2011) The sarcoplasmic reticulum luminal thiol oxidase ERO1 regulates cardiomyocyte excitation-coupled calcium release and response to hemodynamic load. *FASEB J.* **25,** 2583–2591
27. Xiao, R., Wilkinson, B., Solovyov, A., Winther, J. R., Holmgren, A., Lundström-Ljung, J., and Gilbert, H. F. (2004) The contributions of protein disulfide isomerase and its homologues to oxidative protein folding in the yeast endoplasmic reticulum. *J. Biol. Chem.* **279,** 49780–49786
28. Vitu, E., Kim, S., Sevier, C. S., Lutzky, O., Heldman, N., Bentzur, M., Unger, T., Yona, M., Kaiser, C. A., and Fass, D. (2010) Oxidative activity of yeast Ero1p on protein disulfide isomerase and related oxidoreductases of the endoplasmic reticulum. *J. Biol. Chem.* **285,** 18155–18165
29. Weissman, J. S., and Kim, P. S. (1991) Reexamination of the folding of BPTI: predominance of native intermediates. *Science* **253,** 1386–1393
30. Pirneskoski, A., Klappa, P., Lobell, M., Williamson, R. A., Byrne, L., Alanen, H. I., Salo, K. E., Kivirikko, K. I., Freedman, R. B., and Ruddock, L. W. (2004) Molecular characterization of the principal substrate binding site of the ubiquitous folding catalyst protein disulfide isomerase. *J. Biol. Chem.* **279,** 10374–10381
31. Kim, S., Sideris, D. P., Sevier, C. S., and Kaiser, C. A. (2012) Balanced Ero1 activation and inactivation establishes ER redox homeostasis. *J. Cell Biol.* **196,** 713–725
32. Schulman, S., Wang, B., Li, W., and Rapoport, T. A. (2010) Vitamin K epoxide reductase prefers ER membrane-anchored thioredoxin-like redox partners. *Proc. Natl. Acad. Sci. U.S.A.* **107,** 15027–15032
33. Jessop, C. E., Watkins, R. H., Simmons, J. J., Tasab, M., and Bulleid, N. J. (2009) Protein disulphide isomerase family members show distinct substrate specificity: P5 is targeted to BiP client proteins. *J. Cell Sci.* **122,** 4287–4295
34. Braakman, I., Helenius, J., and Helenius, A. (1992) Manipulating disulfide bond formation and protein folding in the endoplasmic reticulum. *EMBO J.* **11,** 1717–1722
35. Mezghrani, A., Fassio, A., Benham, A., Simmen, T., Braakman, I., and Sitia, R. (2001) Manipulation of oxidative protein folding and PDI redox state in mammalian cells. *EMBO J.* **20,** 6288–6296
36. Eletto, D., Chevet, E., Argon, Y., and Appenzeller-Herzog, C. (2014) Redox controls UPR to control redox. *J. Cell Sci.* **127,** 3649–3658
37. Shepherd, C., Oka, O. B., and Bulleid, N. J. (2014) Inactivation of mammalian Ero1α is catalysed by specific protein disulfide-isomerases. *Biochem. J.* **461,** 107–113
38. Nguyen, V. D., Wallis, K., Howard, M. J., Haapalainen, A. M., Salo, K. E., Saaranen, M. J., Sidhu, A., Wierenga, R. K., Freedman, R. B., Ruddock, L. W., and Williamson, R. A. (2008) Alternative conformations of the x region of human protein disulphide-isomerase modulate exposure of the substrate binding b' domain. *J. Mol. Biol.* **383,** 1144–1155
39. Wang, C., Chen, S., Wang, X., Wang, L., Wallis, A. K., Freedman, R. B., and Wang, C. C. (2010) Plasticity of human protein disulfide isomerase: evidence for mobility around the X-linker region and its functional significance. *J. Biol. Chem.* **285,** 26788–26797
40. Solovyov, A., Xiao, R., and Gilbert, H. F. (2004) Sulfhydryl oxidation, not disulfide isomerization, is the principal function of protein disulfide isomerase in yeast *Saccharomyces cerevisiae*. *J. Biol. Chem.* **279,** 34095–34100
41. Appenzeller-Herzog, C., and Ellgaard, L. (2008) *In vivo* reduction-oxidation state of protein disulfide isomerase: the two active sites independently occur in the reduced and oxidized forms. *Antioxid. Redox Signal.* **10,** 55–64